



NRL/MR/6703--15-9610

Guiding Supersonic Projectiles Using Optically Generated Air Density Channels

PHILLIP SPRANGLE

*Directed Energy Physics
Plasma Physics Division*

LUKE A. JOHNSON

*University of Maryland
College Park, Maryland*

March 24, 2015

Approved for public release; distribution is unlimited.

REPORT DOCUMENTATION PAGE

Form Approved
OMB No. 0704-0188

Public reporting burden for this collection of information is estimated to average 1 hour per response, including the time for reviewing instructions, searching existing data sources, gathering and maintaining the data needed, and completing and reviewing this collection of information. Send comments regarding this burden estimate or any other aspect of this collection of information, including suggestions for reducing this burden to Department of Defense, Washington Headquarters Services, Directorate for Information Operations and Reports (0704-0188), 1215 Jefferson Davis Highway, Suite 1204, Arlington, VA 22202-4302. Respondents should be aware that notwithstanding any other provision of law, no person shall be subject to any penalty for failing to comply with a collection of information if it does not display a currently valid OMB control number. PLEASE DO NOT RETURN YOUR FORM TO THE ABOVE ADDRESS.

1. REPORT DATE (DD-MM-YYYY) 24-03-2015		2. REPORT TYPE Interim		3. DATES COVERED (From - To) June 2014 – January 2015	
4. TITLE AND SUBTITLE Guiding Supersonic Projectiles Using Optically Generated Air Density Channels				5a. CONTRACT NUMBER	
				5b. GRANT NUMBER	
				5c. PROGRAM ELEMENT NUMBER	
6. AUTHOR(S) Phillip Sprangle and Luke A. Johnson ¹				5d. PROJECT NUMBER 67-4374-C4	
				5e. TASK NUMBER	
				5f. WORK UNIT NUMBER	
7. PERFORMING ORGANIZATION NAME(S) AND ADDRESS(ES) Naval Research Laboratory 4555 Overlook Avenue, SW Washington, DC 20375-5320				8. PERFORMING ORGANIZATION REPORT NUMBER NRL/MR/6703--15-9610	
9. SPONSORING / MONITORING AGENCY NAME(S) AND ADDRESS(ES) Office of Naval Research 875 North Randolph Street, Suite 1425 Arlington, VA 22203-1995				10. SPONSOR / MONITOR'S ACRONYM(S) ONR	
				11. SPONSOR / MONITOR'S REPORT NUMBER(S)	
12. DISTRIBUTION / AVAILABILITY STATEMENT Approved for public release; distribution is unlimited.					
13. SUPPLEMENTARY NOTES ¹ University of Maryland, College Park, MD 20742-4111					
14. ABSTRACT We investigate the feasibility of using optically generated channels of reduced air density to provide trajectory correction (guiding) for a supersonic projectile. It is shown that the projectile experiences a force perpendicular to its direction of motion as it passes through a channel of reduced air density. This is because the channel's displacement from the projectile's axis of symmetry results in a differential surface pressure. A single channel of reduced air density can be generated by the energy deposited from filamentation of an intense femtosecond laser pulse. We propose changing the laser pulse energy from shot-to-shot to build longer effective channels. We find that current femtosecond lasers systems with multi-millijoules laser pulses could provide trajectory correction of several meters on 5 km trajectories for sub-kilogram projectiles traveling at Mach 2 to Mach 3.					
15. SUBJECT TERMS Guiding supersonic projectiles Optical guide of projectiles Air density channels					
16. SECURITY CLASSIFICATION OF:			17. LIMITATION OF ABSTRACT Unclassified Unlimited	18. NUMBER OF PAGES 15	19a. NAME OF RESPONSIBLE PERSON Phillip Sprangle
a. REPORT Unclassified Unlimited	b. ABSTRACT Unclassified Unlimited	c. THIS PAGE Unclassified Unlimited			19b. TELEPHONE NUMBER (include area code) (202) 767-3493

Guiding Supersonic Projectiles using Optically Generated Air Density Channels

Phillip Sprangle and Luke A. Johnson¹

Plasma Physics Division, Naval Research Laboratory, Washington DC 20375

¹University of Maryland, College Park, Maryland

Abstract

We investigate the feasibility of using optically generated channels of reduced air density to provide trajectory correction (guiding) for a supersonic projectile. It is shown that the projectile experiences a force perpendicular to its direction of motion as one side of the projectile passes through a channel of reduced air density. A single channel of reduced air density can be generated by the energy deposited from filamentation of an intense laser pulse. We propose changing the laser pulse energy from shot-to-shot to build longer effective channels. Current femtosecond lasers systems with multi-millijoules pulses could provide trajectory correction of several meters on 5 km trajectories for sub-kilogram projectiles traveling at Mach 2 to Mach 3.

I. Introduction

The purpose of this paper is to consider the possibility of guiding supersonic projectiles by forming channels of reduced air density in front of the projectile as shown in Fig. 1. A reduced air density region on one side of the projectile would create a surface pressure imbalance, resulting in a net transverse force on the projectile and thus the possibility of trajectory correction, i.e., guiding. Air density channels are formed by creating plasma filaments ahead of the projectile with high-intensity lasers pulses. The plasma filaments consist of hot electrons which collisionally heat the surrounding air forming a density depression. The filaments are generated by a dynamic balancing between the laser's nonlinear self-focusing and plasma defocusing. From shot-to-shot, the location of the laser focus can be controlled by a combination of adjusting the initial conditions of the laser pulse, such as the pulse energy. A flying focus, consisting of successive laser pulses focusing at different locations, can produce air density channels ahead of the projectile over a distance much larger than a single filament.

There is extensive literature on using plasmas for supersonic flow control, specifically for the purpose of drag reduction (Touchard 2008). In these systems, plasmas are generated as either a means to deposit energy and disrupt bow shocks (Kim 2011) or as a means to modify the surface flow and avoid laminar flow separation (Touchard 2008). Our work is distinct from this

body of literature because it is focused on the feasibility of projectile guiding instead of drag reduction. The concept of using laser energy deposition for shock modification and projectile guiding was previously proposed in a U.S. patent (Kremeyer 2003) but the feasibility and physics of the mechanism were not covered.

The paper consists of three sections dealing with a) the degree of projectile deflection given by an air density channel, b) the formation and characteristics of air density channels and finally c) the procedure for forming a flying focus.

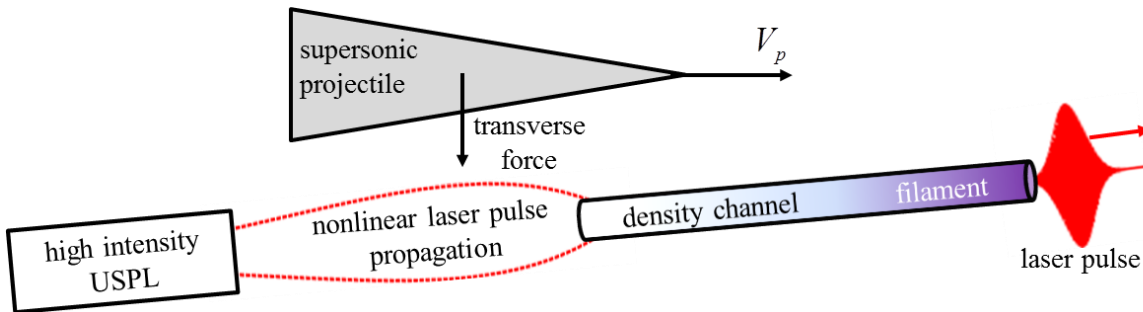


FIG. 1. Configuration of the laser pulse system, plasma filament, and air density channel with respect to the supersonic projectile.

II. Supersonic Projectile Deflection

A. Forces on Projectile

To determine the effect of an air density channel on the projectile’s trajectory, the total force on the projectile must be calculated. As the projectile moves through the air, it is only interacting with the gas through the air pressure over its surfaces. Therefore, in principle, the net force is found by integrating the pressure over the projectile’s surface. When the net force is decomposed into components anti-parallel and perpendicular to the projectile’s direction of motion, it is referred to as the drag and lift, respectively. The force perpendicular to the projectile’s motion will be referred to as the “transverse force” to emphasize that its purpose is for deflecting the projectile and not solely for lift. The projectile’s drag force in the absence of an air density channel will be considered first, then, the effect of the air density channel on the projectile’s net transverse force will be estimated.

The projectile shape is a two-dimensional wedge as shown in Fig. 2. The characteristic transverse length is $\sqrt{A_{\perp}}$ and wedge half-angle is θ . The projectile is assumed to be traveling at

supersonic velocities $V_p > V_s$ where V_s is the sound speed. An oblique shock wave is produced having an angle β with respect to the z axis. The shock angle β is a function of the Mach number M and the wedge half-angle θ . The shock angle is always greater than the Mach angle μ , i.e., $\beta \geq \mu = \sin^{-1}(1/M)$, where the Mach number is given by $M = V_p / V_s$ (Anderson, 1991). For a stable projectile, a body downstream from the wedge is required. The body is neglected because it would have complicated the analysis of the projectile's net forces and detract from the focus of this paper, which is on the characteristic forces from an air density channel on a model projectile.

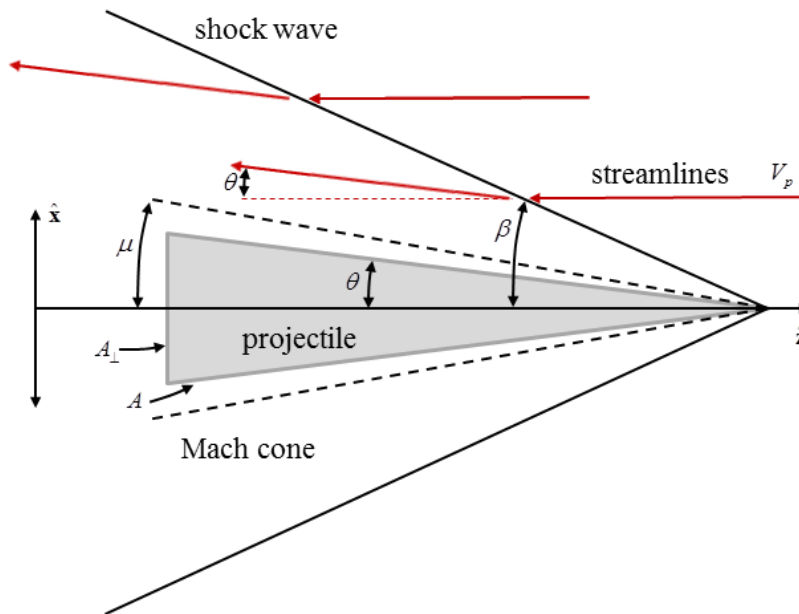


FIG. 2. A two-dimensional wedge projectile shown in the frame moving with the projectile. The Mach cone (dotted black lines), fluid (air) streamlines (red arrows), and shock wave (solid black lines) are also shown.

The air pressure downstream of the shock wave is greater than the ambient air pressure and is responsible for the applied normal forces on the projectile's surfaces. By summing the components of these forces, the drag and transverse force on the projectile can be estimated.

The drag force is defined as $F_D = (C_D / 2) \rho A_{\perp} V_p^2$, where C_D is the drag coefficient, ρ is the mass density of air ($\rho = 1.2 \text{ kg/m}^3$), and A_{\perp} is the characteristic transverse area of the projectile. The drag coefficient is a unitless parameter which captures any additional dependence

the drag force may have on Mach number M , Reynolds number $R_e > 10^3$, and projectile geometry. Typically, for a supersonic projectile, the drag coefficient is $C_D \approx 0.3$ to 0.4 (McCoy 1990).

If the ambient air density is uniform, i.e., no air density channel, the upper (shown in Fig. 2) transverse force is equal in magnitude and opposite in direction of the lower transverse force, and there is no net transverse force on the projectile. There would be a drag force and to estimate it we consider the projectile shown in Fig. 2. The oblique shock relations (Anderson, 1991) in the limit $M^2 \sin^2 \beta \gg 1$, yield a pressure on the upper and lower surfaces of the projectile $p_u = p_l = 2\gamma(\gamma+1)^{-1} p M^2 \sin^2 \beta$, where p is the upstream pressure and $\gamma = 1.4$ is the heat capacity ratio of air. The contributions to the drag force from the upper and lower surfaces are $\mathbf{F}_{D,u} = \mathbf{F}_{D,l} = -p_u A \sin \theta \hat{\mathbf{z}}$, where A is the upper or lower surface area. The net drag force is $F_D = (C_D / 2) \rho A_{\perp} V_p^2$, where the drag coefficient is $C_D = 4(\gamma+1)^{-1} \sin^2 \beta$, the transverse area is $A_{\perp} = 2A \sin \theta$, and the speed of sound is related to the upstream pressure and density via $V_s^2 = \gamma p / \rho$. For air, $C_D = 1.7 \sin^2 \beta$.

If, however, the ambient air mass density ρ has a transverse spatial gradient, such as an air density channel, then the projectile will experience drag and a transverse force. Unfortunately this configuration cannot as easily be analyzed with oblique shock theory and therefore we turn to the Newtonian theory is used to gain intuition about the effect of an air density channel. The Newtonian theory neglects shock formation and calculates the necessary rate of change in momentum to move the air out of the projectile's path. For a wedge in uniform air the drag can be found by using the oblique shock relations and taking the limits of $M \rightarrow \infty$ and $\gamma \rightarrow 1$. As a result, the shock angle limits to the wedge angle, $\beta \rightarrow \theta$, and the drag coefficient becomes $C_D = 2 \sin^2 \theta$ (Anderson 1991). In the case of a density depression of $\Delta\rho$ over a transverse area ΔA on the lower side of the wedge, the Newtonian theory yields a net transverse force of $F_{\perp} = \cot \theta C_D (\Delta\rho / \rho) (\Delta A / A_{\perp}) \rho A_{\perp} V_p^2$ in the direction of the air density channel, where $C_D = 2 \sin^2 \theta$. In order to get an estimate for the characteristic transverse force, we can use a typical drag coefficients of $C_D = 0.3$ (McCoy 1990) to provide an estimate for the effective projectile wedge half-angle $\theta \approx 23^\circ$. To lowest order in $\Delta\rho$ and ΔA , the ratio of the transverse force to the drag is $F_{\perp} / F_D = \cot \theta (\Delta\rho / \rho) (\Delta A / A_{\perp})$, where $\cot \theta \approx 2.4$ to be consistent with

$\theta \approx 23^\circ$. While the fractional change in air density and ratio of air density channel's area to projectile's area are both small, the drag force can be sizable. This will result in significant deflection of the projectile.

B. Transverse Deflection of Projectile

The net transverse force on the projectile will cause deflection towards the air density channel. By assuming that the net transverse force is constant as the projectile passes through the air density channel the deflection can be estimated. A single air density channel will not cause a significant deflection by itself. Therefore, several air density channels will need to be created one after another to build up the transverse velocity of the projectile.

For a single air density channel, the transverse velocity of the projectile $v_\perp(t)$ is given by $m_p \dot{v}_\perp = F_\perp$, where m_p is the projectile mass and F_\perp is the net transverse force due to the air density channel. As will be shown, the initial laser pulses can be changed from shot-to-shot to create an extended air density channel that is formed from N_c single channels joined end-to-end. The change in the transverse velocity Δv_\perp , at the end of a sequence of N_c air density channels, each of length L_c , is $\Delta v_\perp = (F_\perp/m_p)(N_c L_c/V_p)$. Note that in general, the channels do not have to be connected end-to-end but could have an arbitrary spacing.

After propagating a distance L from the start of the air density channel, the transverse displacement of the projectile is $\Delta x_\perp = \Delta v_\perp(L - N_c L_c/2)/V_p$, where $L \geq N_c L_c$. When the estimate of the net transverse force is used, the deflection of the projectile is given in terms of channel and projectile parameters

$$\Delta x_\perp = \frac{C_D}{2} \left(\frac{\Delta \rho}{\rho} \right) \left(\frac{\Delta A}{A_\perp} \right) \left(\frac{\rho A_\perp N_c L_c}{m_p} \right) \left(L - \frac{N_c L_c}{2} \right). \quad (1)$$

As an example of the amount of transverse displacement a projectile can develop we consider the parameters; $\Delta \rho/\rho = 0.1$, $\Delta A/A_\perp = 0.01$, $C_D = 0.3$, $m_p = 100\text{g}$, $A_\perp = 4\text{cm}^2$, $N_c = 20$, $L_c = 40\text{m}$, and $L = 5\text{km}$. The resulting transverse displacement is $\Delta x_\perp = 2.9\text{m}$. For comparison, the deflection after just the first air density channel in that sequence would be $\Delta x_\perp = (C_D/2)(\Delta \rho/\rho)(\Delta A/A_\perp)(\rho A_\perp L_c/m_p)(L_c/2) = 0.6\text{mm}$.

III. Air Density Channel Formation

Formation of the air density channels occurs in a four step process (Cheng 2013, Jhajj 2014). First, an ultrashort laser pulse deposits energy in the air via multiphoton ionization. Second, the free electrons redistribute the energy gained when ionized as heat by colliding with neutrals and attaching to oxygen molecules. The local heating of the air occurs much faster (nanoseconds) than the energy can be carried away by acoustic waves (microseconds). As a result, the third step is the formation of a pressure shock wave. Finally, after the region has reached uniform pressure, the remaining thermal energy has an associated air density channel which thermally diffuses on millisecond timescales.

The deposition of laser energy in the air occurs over distances larger than a Rayleigh length because of laser filamentation. Filamentation is the result of a dynamic balancing of the focusing effect of the nonlinear Kerr index and the defocusing effect of the laser generated plasma (Couraion 2007). Due to this balancing, the laser intensity and plasma density in an air filament are clamped to approximately $10^{13} - 10^{14} \text{ W/cm}^2$ and $1 - 5 \times 10^{16} \text{ cm}^{-3}$, respectively (Couraion 2007). Typical electron energies in a filament are $1 - 2 \text{ eV}$ (Couraion 2007). The lifetime of the plasma due to attachment is approximately 10 ns . This translates into plasma filaments which at any moment are approximately 3 m in length. These filamentation parameters are typical and have been observed both experimentally and numerically. They will be used when making estimates that depend on the filament's properties.

The details of the laser's filamentation (Sprangle 2002) and air's hydrodynamic expansion (Cheng 2013, Jhajj 2014) have been discussed in previous works. Of key importance to projectile guiding, are estimates of the magnitude (ΔN_{air}), volume ($\pi R_c^2 L_c$), and duration (τ_{diff}) of the air channel's density depression and the resulting requirements placed on the laser pulses.

To estimate the magnitude of the air density depression, first note that for an ideal gas at constant pressure the change in air number density ΔN_{air} is proportional to the local change in air temperature ΔT_{air} , that is, $\Delta N_{\text{air}} = -N_{\text{air}} \Delta T_{\text{air}} / T_{\text{air}}$, where the total number density and temperature are given by $N_{\text{air}} + \Delta N_{\text{air}}$ and $T_{\text{air}} + \Delta T_{\text{air}}$. Estimating the increase in air temperature due to electron heating will provide an estimate for the magnitude of the air density depression. For a gas species in thermodynamic equilibrium each accessible degree of freedom (translational, vibrational and

rotational) has a kinetic or potential energy of $k_B T_{\text{air}} / 2$, where k_B is the Boltzmann constant. Therefore, each electron and air molecule have a thermal energy of $3k_B T_e / 2$ and $5k_B T_{\text{air}} / 2$, respectively. Suppose that all of the electron's thermal (internal) energy is transferred to the air. The change in air temperature due to electron heating is $(5/2)N_{\text{air}}k_B\Delta T_{\text{air}} = \Delta U_{\text{air}}$, where the energy deposited in the air is $\Delta U_{\text{air}} = (3/2)N_e k_B T_e$. The fractional change in air temperature is $\Delta T_{\text{air}} / T_{\text{air}} = (3/5)(N_e / N_{\text{air}})T_e / T_{\text{air}} \approx 0.085$ for $T_e = 2\text{eV}$, $T_{\text{air}} = 0.026\text{eV}$, $N_e = 5 \times 10^{16} \text{cm}^{-3}$, and $N_{\text{air}} = 2.7 \times 10^{19} \text{cm}^{-3}$. The resulting fractional change of the air density in a channel is $\Delta N_{\text{air}} / N_{\text{air}} \approx -0.085$.

To generated air density channels with a sufficient density depression ΔN_{air} for projectile guiding, enough laser energy will need to be deposited locally to heat the air. This sets a lower bound on the necessary laser pulse energy $E_{\text{laser, min}}$. As previously mentioned, the temperature change in a gas is related to the thermal (internal) energy by $\Delta E = (5/2)N_{\text{air}}k_B\Delta T_{\text{air}}$ and any changes in air temperature will be accompanied by a change in air density $\Delta N_{\text{air}} / N_{\text{air}} = -\Delta T_{\text{air}} / T_{\text{air}}$. Therefore, the thermal energy change in a single air density channel is proportional to the air density depression such that $\Delta E = (5/2)N_{\text{air}}k_B T_{\text{air}} (-\Delta N_{\text{air}} / N_{\text{air}})(\pi R_c^2 L_c)$, where R_c and L_c are the channel radius and length. Typical channel dimensions, as will be discussed, are $L_c = 40\text{m}$ and $R_c = 0.02\text{cm}$. In order to achieve a 10% depression in the air density ($\Delta N_{\text{air}} / N_{\text{air}} = -0.1$), the thermal energy must increase by $\Delta E = 140\text{mJ}$. This sets a lower bound on the required laser pulse energy $E_{\text{laser, min}} \geq 140\text{mJ}$ and is achievable with current laser systems (Stelmaszczyk 2004).

The air density channel's length will always be less than the maximum propagation length of the filament L_{max} . By using the energy depletion length of the filament, an upper bound on the air density channels length can be estimated. This and the characteristic channel radius of $R_c = 0.02\text{cm}$ (Cheng 2013) provide an estimate for the volume of the air density channel $\pi R_c^2 L_c$. The maximum propagation distance of a laser pulse generating a filament is limited by energy depletion from ionization of the air (Sprangle 2002). If all of the laser pulse energy goes to ionizing the gas, this distance is approximately $L_{\text{max}} = E_{\text{laser}} / (U_{\text{ion}} N_e \pi R_c^2)$. For a laser energy of $E_{\text{laser}} = 140\text{mJ}$ and typical atmospheric filamentation parameters, such as an ionization energy of

$U_{\text{ion}} = 12\text{eV}$, electron density of $N_e = 5 \times 10^{16} \text{cm}^{-3}$, and filament radius of $R_f = 0.01\text{cm}$ (Courairon 2007), the maximum propagation distance of a single laser pulse undergoing filamentation is $L_{\text{max}} = 46\text{m}$.

Finally, there are several relevant timescales to consider. The first is the timescale for collisionally heating of the air channel by the electrons (Tzortzakis 2001, Cheng 2013). The transfer of electron kinetic energy to the neutral gas occurs via electron-neutral collisions and the collision time is $\tau_c \sim 1\text{ps}$. As a result, the air channel heating time τ_h is approximately the electron-to-neutral mass ratio times the electron-neutral collision time τ_c , that is, $\tau_h = (M_n / m_e) \tau_c \sim 50\text{ns}$, where the neutral mass is $M_n \approx 5 \times 10^{-26} \text{kg}$. This is comparable to the time scale of electron attachment to oxygen and it is expected that the heating mechanism depends on both processes. The air density depression develops on the time scale that the pressure equilibrates, that is, $\tau_{\text{dev}} \sim R_c / V_s = 0.7 \mu\text{s}$, where the speed of sound is $V_s = 300 \text{m/s}$ and $R_c = 200 \mu\text{m}$. The air channel life time is set by the thermal diffusion $\tau_{\text{diff}} \sim R_c^2 / D = 1.5\text{ms}$, where the diffusion coefficient of air is $D = 27 \text{mm}^2 / \text{s}$ (Cheng 2013) and $R_c = 200 \mu\text{m}$.

As an aside, the electron's mean free path is small compared to the radius of the filament implying that the filament and air channel have approximately the same radius. This is consistent with experimental observations (Cheng 2013, Courairon 2007).

IV. Flying Focus

The concept of projectile guiding using air channels relies on the generation of many air density channels along the projectile's trajectory. As discussed previously, the characteristic lifetime of the air density channel is a millisecond. For a projectile velocity of Mach 3, the air channels must be formed no farther than several meters in front of the projectile or else the air density channel will have dissipated before the projectile arrives. Consequently, the plasma filaments and the resulting air density channels must move from shot-to-shot at the projectile velocity.

As a generalization of the terminology of Gaussian optics, the initial location at which the laser pulse collapses into a plasma filament will be referred to as the focus. The movement of the focus from shot-to-shot will similarly be referred to as the "flying focus."

Linear and nonlinear laser pulse propagation provides numerous mechanisms for controlling the laser pulse focus or filamentation location, such as focusing, frequency chirp, or pulse energy. By controlling the initial laser pulse parameters from shot-to-shot, the focal point of the laser can be moved and thereby create a flying focus. There has been ample theoretical and experimental work on ultrashort laser pulse propagation and the generation of filaments in the atmosphere (Sprangle 2002, Couairon 2007, Berge 2007). This section follows the methods of previous work (Sprangle 2002) in solving for the propagation of an ultrashort laser pulse in the atmosphere.

The flying focus concept considered here relies on propagation of intense laser beams in the atmosphere. This propagation is strongly affected by various interrelated linear and nonlinear processes (Sprangle 2002). These include diffraction, Kerr self-focusing, group velocity dispersion, spectral broadening, self-phase modulation, and turbulence. In general, a laser pulse propagating in air can be focused longitudinally and transversely at remote distances (\sim km) to reach high intensities ($\sim 10^{13}$ W/cm²). Due to group velocity dispersion, temporal pulse compression can be achieved by introducing a frequency chirp on the pulse. Nonlinear transverse self-focusing is caused by the optical Kerr effect. Essential to filamentation is that the transverse self-focusing leads to a collapse in the laser spot size.

A model describing the longitudinal and transverse compression of a chirped laser pulses in air will be presented (Sprangle 2002). This model uses an extension of the paraxial wave equation with the assumption that the laser pulse maintains a Gaussian shape, both transversely and temporally, as it propagates. From these assumptions, a set of coupled differential equations for the laser spot size and temporal duration have been derived. Additional details can be found in reference (Sprangle 2002).

The laser electric field is given by $\mathbf{E}(r, \eta, \tau) = \hat{E}(r, \eta, \tau) \exp[i\Delta k\eta - i\omega\tau] \hat{\mathbf{e}}_x / 2 + c.c.$, where \hat{E} is the complex amplitude, ω is the frequency, k is the wavenumber, $\Delta k = k - \omega/c$ is the wavenumber shift from air's linear dispersion relation, r is the radial coordinate, and $\tau = t - z/c$ and $\eta = z$ are the light frame coordinates. The propagation distance z and time t are in the laboratory frame. The complex field amplitude is assumed to be a transverse and temporal Gaussian $\hat{E}(r, \eta, \tau) = A_o(\eta) \exp[i\theta(\eta)] \exp[-(1 + i\alpha(\eta))r^2 / R^2(\eta)] \exp[-(1 + i\beta(\eta))\tau^2 / T^2(\eta)]$ where $A_o(\eta)$ is the field amplitude, $\theta(\eta)$ is the phase, $R(\eta)$ is the spot size, $\alpha(\eta)$ is related to

the curvature of the wavefront, $T(\eta)$ is the laser pulse duration, and $\beta(\eta)$ is the chirp parameter. The quantities A_0 , θ , T , R , α , and β are real functions of the propagation distance. As shown in reference (Sprangle 2002), the following coupled equations for R and T are obtained,

$$\frac{\partial^2 R}{\partial \eta^2} = \frac{4}{k^2 R^3} \left(1 - \frac{E_o}{P_{NL}} \frac{1}{T} \right), \quad (2a)$$

$$\frac{\partial^2 T}{\partial \eta^2} = \frac{4\beta_2}{k} \frac{E_o}{P_{NL}} \frac{1}{R^2 T^2} + \frac{4\beta_2^2}{T^3}, \quad (2b)$$

where $E_o = P(0)T(0)$ is proportional to the laser pulse energy and is independent of η , $P(\eta) = \pi R^2(\eta)I(\eta)/2$ is the laser power, $I(\eta) = cA_o^2(\eta)/(8\pi) = I(0)R^2(0)T(0)/[R^2(\eta)T(\eta)]$ is the peak intensity, $P_{NL} = \lambda^2/(2\pi n_K)$ is the self-focusing or critical power, and β_2 is the group velocity dispersion. For air at STP and wavelength $\lambda = 2\pi/k \approx 1\mu\text{m}$, the group velocity dispersion is $\beta_2 = 2.2 \times 10^{-31} \text{s}^2/\text{cm}$, the Kerr nonlinear index is $n_K = 3 \times 10^{-19} \text{cm}^2/\text{W}$, and $1 + n_K I$ is the refractive index of air. The instantaneous frequency shift along the pulse, i.e., chirp, is $\delta\omega(\eta, \tau) = 2\beta(\eta)\tau/T^2(\eta)$, where $\beta(\eta) = T(\eta)/(2\beta_2)\partial T(\eta)/\partial \eta$. A negative (positive) frequency chirp, $\beta(\eta) < 0$ ($\beta(\eta) > 0$), results in decreasing (increasing) frequencies towards the back of the pulse. Similarly, the wavefront curvature is related to $\alpha(\eta) = -(kR(\eta)/2)\partial R(\eta)/\partial \eta$ with a focusing (defocusing) laser field corresponding to $\alpha(\eta) > 0$ ($\alpha(\eta) < 0$). The initial conditions of Eqs. (2) and subsequent evolution of R and T are determined by the initial laser spot size $R(0)$, focusing or defocusing via $\alpha(0)$, pulse duration $T(0)$, and frequency chirp via $\beta(0)$.

The first term on the right hand side of Eq. (2a) describes vacuum diffraction while the second term describes nonlinear self-focusing, i.e., due to n_K . Nonlinear self-focusing dominates diffraction resulting in filamentation when $P > P_{NL} \approx 3\text{GW}$ (Sprangle 2002), Couairon 2007).

In general, the laser pulse's spatiotemporal shape will not remain Gaussian, but this approximation is acceptable during the propagation leading up to filamentation (see Fig. 10 of reference [Sprangle 2002]). After filamentation, the laser pulse may or may not be Gaussian and ionization would need to be included in the model, but this paper is only interested in the location

where the plasma filament begins. Therefore, solving Eqs. (2) is sufficient for determining feasibility of the flying focus.

In the limit that the pulse length does not change appreciably the laser spot size is given by $R(\eta) = R(0) \left[1 - 2\alpha(0)\eta / Z_{R0} + (\alpha^2(0) + 1 - P / P_{NL})(\eta / Z_{R0})^2 \right]^{1/2}$, where $Z_{R0} = kR^2(0) / 2$ is the Rayleigh length in the absence of initial- or self-focusing, that is $\alpha(0) = 0$ and $P_{NL} \rightarrow \infty$. This is similar to Gaussian optics. The spot size collapses to zero, $R(\eta_c) = 0$, at a distance $\eta_c / Z_{R0} = \left(\alpha(0) - \sqrt{P / P_{NL} - 1} \right) / \left(\alpha^2(0) + 1 - P / P_{NL} \right)$ under the conditions that either $(1 + \alpha^2(0))P_{NL} > P > P_{NL}$ for $\alpha(0) > 0$ or $P > (1 + \alpha^2(0))P_{NL}$ for all $\alpha(0)$.

A similar analysis can treat the laser pulse duration without self-focusing ($P_{NL} \rightarrow \infty$) $T(\eta) = T(0) \sqrt{(1 + \beta(0)\eta / Z_T)^2 + (\eta / Z_T)^2}$, where the chirp parameter $\beta(0)$ is like the initial temporal focusing or defocusing, and the group velocity length $Z_T = T^2(0) / (2|\beta_2|)$ is like the temporal Rayleigh length.

For example, the start of the plasma filament is shown as a function of laser pulse energy in Fig. 3. In the ideal case, when $T(\eta) = T(0)$, the collapse point of the laser spot goes off to infinity as the pulse power approaches the critical power, i.e. 0.6 mJ for a 200 fs pulse. Equations (2) do reproduce the result of $z = Z_{R0} / \sqrt{P / P_{NL} - 1}$ for $P > P_{NL}$ when $\alpha(0) = 0$, but when the temporal spreading of the pulse is included, higher pulse energies are required for the pulse to collapse at the same propagation distance. With temporal spreading, the minimum energy for filamentation is approximately three times larger. The collapse point of the laser pulse can be moved approximately 0.5 km by changing the pulse energy several millijoules.

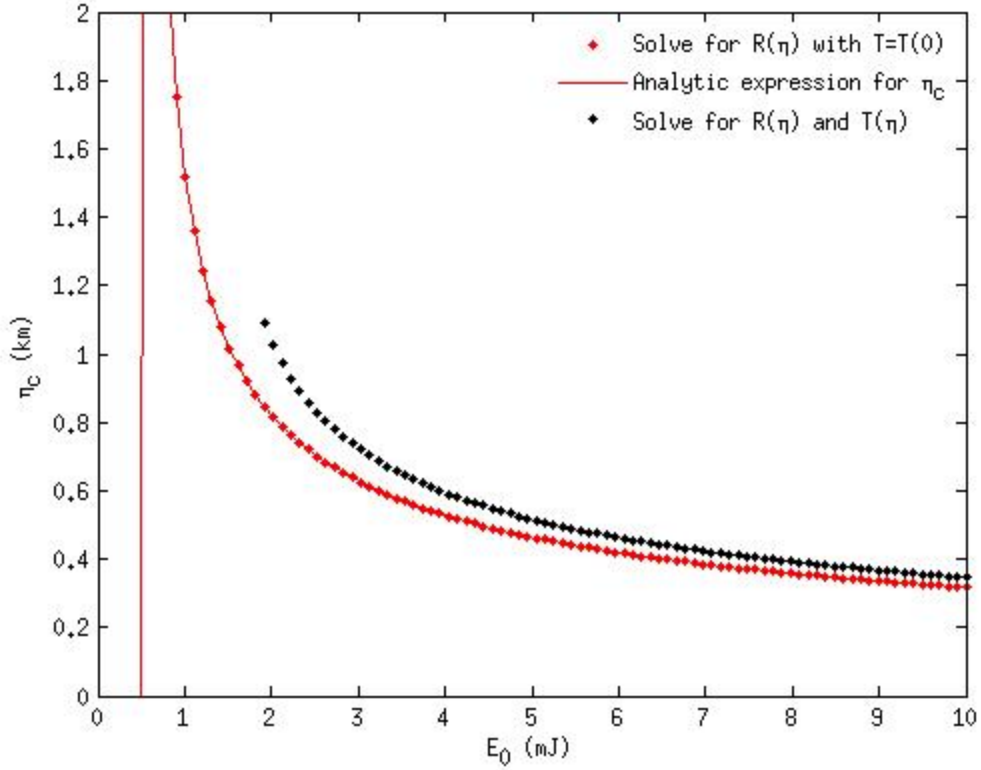


FIG 3. The filamentation location (or collapses point) η_c as a function of laser pulse energy for $T(0) = 200$ fs, $R(0) = 2$ cm, $\alpha(0) = 0$, $\beta(0) = 0$, and $\lambda = 1\mu\text{m}$. The red dots show the numerical solutions of Eqs. (2) and the red solid line is the analytic expression for η_c when $T = T(0)$ and $P > P_{NL}$. The black dots show the numerical solutions of Eqs. (2) when $T(z)$ is allowed to evolve.

The flying focus concept essentially relies on changing the initial conditions of the laser pulse, either the initial energy E_0 , focusing $\alpha(0)$, chirp parameter $\beta(0)$, pulse duration $T(0)$, or spot size $R(0)$, from one laser shot to the next. How fast the flying focus can be moved will depend on how sensitive the filamentation point is to the initial conditions and on how quickly the initial conditions can be changed in the laser system. For example, if the laser pulse energy is changed shot-to-shot and we neglect GVD ($T(z) \approx T_0$), the flying focus velocity would be given by $v_c = (d\eta_c / dE_0)(dE_0 / dt)$.

For projectile guiding, the desired flying focus velocity is ~ 1 km/s. For a 100Hz laser system, the filaments collapse point will have to move 10 m per shot. This could be achieved by

operating a laser system near $E_0 \approx 6$ mJ for the parameters used in Fig. 3. Near this energy the rate of change of the filamentation point is $d\eta_c / dE_0 \approx 45$ m/mJ. The laser system would need to be able to change the pulse energy by 0.2 mJ/shot.

One mechanism for experimentally controlling the laser pulse energy is using a half-wave plate and thin film polarizer. The main objective of a system like this is to take the laser pulse after the last laser amplifier and dump the energy that is not needed. For example, assume that the maximum laser pulse energy that the system can achieve is $E_{0,\max}$. The half-wave plate is a birefringent crystal. If the crystal's length is properly chosen, then the relative phase delay between the components of the field along the crystal's optical axes will cause the laser field polarization to be rotated by 2θ , where θ is the angle between the initial laser polarization and the crystal's fast axis. A thin-film polarizer is then used to separate out one polarization and create a linearly polarized pulse with a smaller desired energy relative to the maximum that the system can achieve, that is $E_0 = \cos^2 \theta E_{0,\max}$.

For example, to achieve a change in laser pulse energy of 0.2 mJ/shot, the half-wave plate can be rotated at the rate of 5.5 RPM near the angle $\theta \approx \pi/3$. The laser system would need to have peak pulse energies of $E_{0,\max} = 20$ mJ, to create 5 mJ pulses in this configuration. This is approximately what would be needed to create a flying focus at Mach 3 near 5 mJ.

V. Conclusions

In conclusion, we have detailed the mechanisms for guiding a supersonic projectile using optically generated air density channels. An estimate of the transverse force and deflection experienced by the projectile passing through air density channel is given. We have outlined the physical processes that are important to the formation of a channel of reduced air density. Additionally, a method for creating extended air density channels by using a flying focus was proposed.

Acknowledgments

This work was supported by Naval Research Laboratory and the Joint Technology Office. The authors would like to thank K. Ryan, E. Rosenthal and A. Ting for useful discussions.

References

- J. D. Anderson, *Fundamentals of Aerodynamics* (McGraw-Hill, Inc., New York, 1991), pp. 1–772.
- L. Bergé, S. Skupin, R. Nuter, J. Kasparian, and J-P Wolf. *Rep. Prog. Phys.* 70 1633 (2007).
- Y. Cheng, J. Wahlstrand, N. Jhajj, and H. Milchberg, *Opt. Express* 21, 4740-4751 (2013).
- A. Couairon and A. Mysyrowicz, *Phys. Rep.* **441**, 47 (2007).
- P. Gnemmi and C. Rey, *J. Spacecr. Rockets* 46, 989 (2009).
- P. Gnemmi, R. Charon, J.-P. Dupéroux, and A. George, *AIAA J.* 46, 1308 (2008).
- N. Jhajj, E. W. Rosenthal, R. Birnbaum, J. K. Wahlstrand, and H. M. Milchberg, *Phys. Rev. X* 4, 011027 (2014).
- K. Kremeyer, Shock wave modification method, apparatus, and system, US Patent, 6,527,221, Mar. 4, 2003.
- R. L. McCoy, *The Aerodynamic Characteristics of .50 Ball M33, API, M8, and APIT, M20 Ammunition* (No. BRL-MR-3810) (pp. 1–83). Aberdeen, Maryland, (1990).
- P. Sprangle, J. Peñano, and B. Hafizi, *Phys. Rev. E* 66, 046418 (2002).
- K. Stelmaszczyk, P. Rohwetter, G. Méjean, J. Yu, E. Salmon, J. Kasparian, R. Ackermann, J.-P. Wolf, and L. Wöste, *Appl. Phys. Lett.* 85, 3977 (2004).
- G. Touchard, *Int. J. Plasma Environ. Sci. Technol.* 2, 1 (2008).
- S. Tzortzakis, B. Prade, M. Franco, A. Mysyrowicz, S. Hüller, and P. Mora, *Phys. Rev. E* 64, 057401 (2001).